Journal of Statistical Physics, Vol. 64, Nos. 3/4, 1991

Disks vs. Spheres: Contrasting Properties of Random Packings

Boris D. Lubachevsky,[1] Frank H. Stillinger,[1] and Elliot N. Pinson[1]

Received March 12, 1991

Collections of random packings of rigid disks and spheres have been generated by computer using a previously described concurrent algorithm. Particles begin as infinitesimal moving points, grow in size at a uniform rate, undergo energy-nonconserving collisions, and eventually jam up. Periodic boundary conditions apply, and various numbers of particles have been considered ($N \leqslant 2000$ for disks, $N \leqslant 8000$ for spheres). The irregular disk packings thus formed are clearly polycrystalline with mean grain size dependent upon particle growth rate. By contrast, the sphere packings show a homogeneously amorphous texture substantially devoid of crystalline grains. This distinction strongly influences the respective results for packing pair correlation functions and for the distributions of particles by contact number. Rapidly grown disk packings display occasional vacancies within the crystalline grains; no comparable voids of such distinctive size have been found in the random sphere packings. "Rattler" particles free to move locally but imprisoned by jammed neighbors occur in both the disk and sphere packings.

KEY WORDS: Rigid disks; rigid spheres; random packings; amorphous solids; rattler particles; vacancies; grain boundaries.

1. INTRODUCTION

Motivated by a wide variety of applications in the physical and biological sciences, many investigations of random disk and sphere packings have found their way into the scientific literature. While some of these studies can be classified as experimental, the recent activity has strongly been biased in favor of computer simulation. The present paper fits this latter description, and extends the work reported in a predecessor.[1]

This paper is dedicated to Jerry Percus on the occasion of his 65th birthday.

[1] AT&T Bell Laboratories, Murray Hill, New Jersey 07974.

0022-4715/91/0800-0501$06.50/0

In a broad sense, two types of packing constructions exist, the "sequential" methods[2–8] and the "concurrent" methods.[1,9–11] The first of these typically begins with small "seed," a fixed arrangement of particles, which then grows by addition of further particles one by one until a large aggregate has been formed. The algorithm used for placing particles in contact with those already present can either be deterministic or stochastic. By contrast, the concurrent methods have the entire collection of particles present from the outset, and utilize some appropriate procedure for arranging them finally into a jammed configuration. One of the important objectives is establishing the statistical differences between packings produced by these various methods.

Our earlier paper[1] presented a concurrent method for generating rigid particle packings. Its basic concept was to start with a random collection of points, assign them random velocities, and grow them at a uniform rate into the repelling particles of interest until jamming occurred. Programming advances in design of event-driven algorithms[12] permitted effective implementation of this packing model for relatively large numbers of particles. This prior study focused on the two-dimensional case, i.e., rigid disks in the plane. One of its surprising results was the frequent observation of "rattler" disks in the packings, namely particles trapped but unjammed in a cage of tightly jammed neighbors. This is a feature not expected nor observed to occur in disk packings produced by sequential methods.

Our primary objective now is to apply our concurrent particle-growth model to the case of rigid spheres in three dimensions. This provides the opportunity to identify similarities and contrasts with the two-dimensional disk packings. In particular it is obvious to search for "rattler" spheres.

Section 2 is devoted to some general remarks that provide a mathematical background for the computations. Section 3 recounts details of our concurrent method for generating rigid particle packings. Section 4 contains some new results for random disk packings that extend (but are consistent with) those of ref. 1. Sphere packing results appear in Section 5, along with commentary about comparisons with the disk case. The closing Section 6 summarizes conclusions, describes some feasible extensions, and indicates some important open problems.

2. GENERAL REMARKS

Consider a set of N identical D-dimensional spheres ($D = 1, 2, 3, \ldots$) confined to a rectangular region with size $L_1 \times L_2 \times \cdots \times L_D$. Let a denote the common sphere diameter. We will demand that periodic boundary conditions apply in each of the D directions. Positions of sphere centers will be denoted by $\mathbf{r}_1 \cdots \mathbf{r}_N \equiv \mathbf{R}$, where $\mathbf{R}$ is a DN-dimensional vector.

In the following we shall be concerned about the set $S(a)$ of nonoverlap configurations $\mathbf{R}$ for the N spheres, i.e., those configurations for which all pair distances are at least a:

$$|\mathbf{r}_i - \mathbf{r}_j| \geqslant a \tag{2.1}$$

Here index i runs over all N particles in Ω_D, while j runs over those particles *and* their periodic images in the $3^D - 1$ contiguous cells. The content (measure) of the allowed region $S(a)$ in the DN-dimensional configuration space

$$C[S(a)] \tag{2.2}$$

is the subject of equilibrium statistical mechanics for the rigid particle systems. In particular it determines the equation of state[13,14] and hence it is fundamental to the existence of fluid–solid phase transitions.

Obviously the content (2.2) is $(\Omega_D)^N$, when $a = 0$, and declines monotonically with increasing a, vanishing finally when $a = a_{\max}$, the largest common diameter that permits all N particles to be packed in Ω_D without overlaps. This maximal diameter $a_{\max}$ will depend generally on all relevant parameters N, D, and the dimensions of Ω_D. However, the fraction ξ of Ω_D covered by these particles

$$\begin{aligned} \xi &= N s_D(a)/\Omega_D \\ s_D(a) &= \pi^{D/2} a^D / 2^D \Gamma(1 + D/2) \end{aligned} \tag{2.3}$$

is subject to the following upper bounds[1]:

$$\begin{aligned} \xi &\leqslant 1 && (D = 1) \\ &\leqslant \frac{\pi}{2\sqrt{3}} = 0.906899\ldots && (D = 2) \\ &\leqslant \frac{\pi}{3\sqrt{2}} = 0.740480\ldots && (D = 3) \end{aligned} \tag{2.4}$$

The particle configurations represented by $S(a_{\max})$ consist of the densest possible packing(s) for the given N, D, and Ω_D, but unless N is very small, this is but a minor fraction of all possible packings. The other, less efficient (smaller ξ), packings are associated with disconnections of $S(a)$ with increasing a. Such disconnections constitute trapping of the system in small portions of the configuration space due to the nonoverlap restrictions (2.1), with consequent loss of dynamical ergodicity. Each disconnected portion may itself undergo further fragmentation with increasing a, but

eventually any fragment shrinks to vanishing content at some characteristic $a = a_p$, corresponding to a particle packing p at common diameter a_p.

A useful definition of particle (line, disk, sphere, ...) packing is the following.

Rigid particle packing: Geometrical arrangement of N nonoverlapping rigid particles in D dimensions for which the available continuous displacements permit fewer then DN degrees of translational freedom.

Put more colloquially, the particles are jammed. On account of the periodic boundary conditions, the number of remanent translational degrees of freedom f is at least D; the presence of n mutually isolated rattlers in the packing would increase f to $(n+1)D$.

One significant way to classify disk or sphere packings is by the network of pair contacts, that is, the set of particle pairs for which $|\mathbf{r}_i - \mathbf{r}_j| = a_p$. In order for a packing to satisfy the above definition, it is necessary for the graph of contact bonds to be above the critical percolation threshold; uninterrupted paths along such bonds must exist threading the fundamental cell Ω_D and its periodic images in all directions. Some particles, specifically the rattlers, may be disconnected from this contact-bond network.

In any given packing p, the number of contacts experienced by particle i will be denoted by $Z_i(p)$. This set of numbers will include contacts within Ω_D as well as contacts across boundaries into the contiguous periodic images of Ω_D. We have the following obvious steric constraints:

$$\begin{aligned} Z_i &\leqslant 2 \qquad (D=1) \\ &\leqslant 6 \qquad (D=2) \\ &\leqslant 12 \qquad (D=3) \end{aligned} \tag{2.5}$$

All Z_i attain the upper limits shown if the packing is a close-packed crystal (gapless array in $D=1$, triangular crystal in $D=2$, face-centered cubic crystal or its stacking variants in $D=3$). A necessary, but certainly not sufficient, condition for particle i to be jammed is given by

$$Z_i(p) \geqslant D+1 \tag{2.6}$$

One also concludes that the number $f(p)$ of remanent translational degrees of freedom for packing p must obey

$$f(p) \geqslant DN - \frac{1}{2}\sum_{i=1}^{N} Z_i(p) \tag{2.7}$$

Figures 1 and 2 provide an illuminating pair of configurations for rigid disks. Both amount to triangular close-packed crystals with one-fourth of the disks missing. With appropriate choices for the cell side lengths L_1 and L_2 these configurations could be commensurate with the periodic boundary conditions imposed. For both cases all particles experience exactly four contacts. Both of these patterns would be stable packings if enclosed by impenetrable walls. But with periodic boundary conditions they are unstable: in Fig. 1 vertical columns two disks wide can move vertically to free up the entire assembly, while diagonal lines of disks (as shown) can do the same

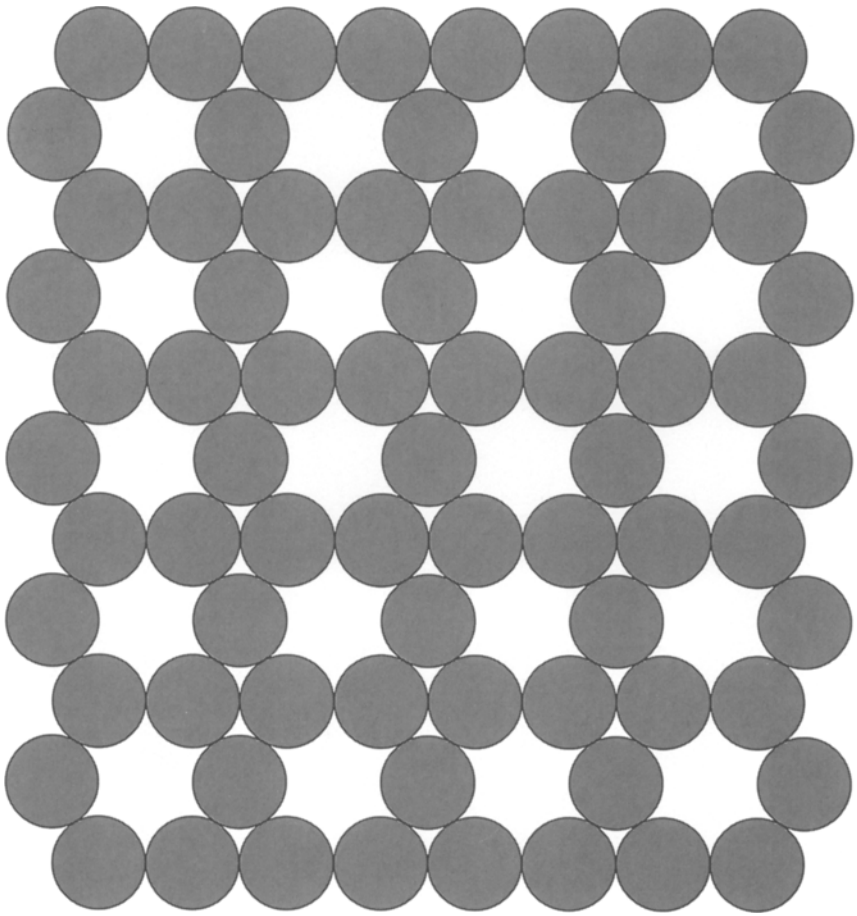

Fig. 1. Low-density arrangement of disks, each one of which contacts four others. The density is three-fourths that of the vacancy-free triangular crystal.

in Fig. 2. However, note that plugging a single horizontal row of vacancies in either pattern with disks eliminates the instability. In a very large system this plugging would have negligible effect on the covering fraction ξ. Clearly the contact numbers alone do not allow one to conclude that a configuration is a valid packing.

Substantial interest resides in the large-system-limit properties of the packings. In particular, the density distribution of random packings has attracted attention. Suppose $P(\xi \mid D, N, L, \varepsilon)$ is the probability for attaining (within $\pm\varepsilon$) covering fraction ξ in packings generated by some construc-

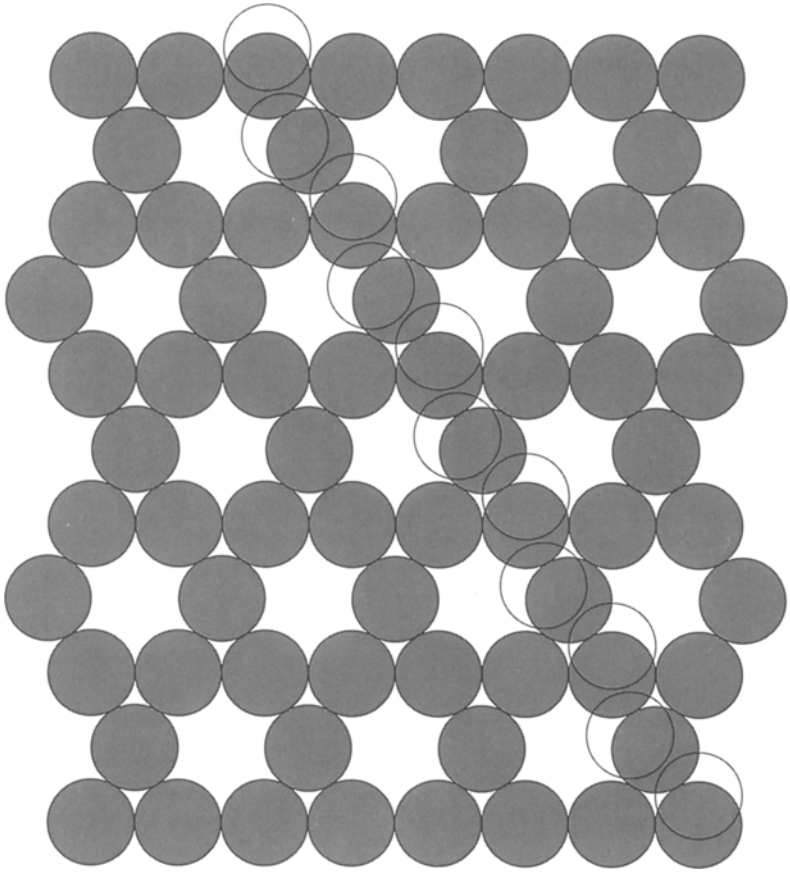

Fig. 2. An alternative disk arrangement which, like that in Fig. 1, has density equal to three-quarters of the maximum possible. This configuration is unstable with respect to the type of displacement shown, and therefore is not a packing.

tion procedure, for N D-spheres in a hypercube with sides L. The limiting distribution then is

$$P_\infty(\xi \mid D) = \lim_{\varepsilon \to 0} \lim_{N, L \to \infty} P(\xi \mid D, N, L, \varepsilon) \tag{2.8}$$

For most "reasonable" construction algorithms one expects the limit distribution to be infinitely narrow:

$$P_\infty(\xi \mid D) = \delta(\xi - \xi_0) \tag{2.9}$$

i.e., a Dirac delta function centered about an algorithm-dependent covering fraction ξ_0. We suspect (but have not proved) that the patterns in Figs. 1 and 2 provide the greatest lower bound on disk packing density, so in $D = 2$ we should find

$$\frac{\pi\sqrt{3}}{8} \leqslant \xi_0 \leqslant \frac{\pi}{2\sqrt{3}} \qquad (D = 2) \tag{2.10}$$

A corresponding lower limit for ξ_0 in $D = 3$ is not known to us at present.

3. CONCURRENT CONSTRUCTION METHOD

Our procedure for generating random particle packings was described in considerable detail in ref. 1, to which the reader is referred for additional information. Its principal features are the following. The basic cell Ω_D is given the same size in each direction, and N points are initially ($t = 0$) placed randomly within its interior with a uniform distribution. These points are given initial velocities whose components are uniformly distributed between -1 and $+1$. As time t increases, the N particles grow at a common rate into rigid lines, disks, spheres, ...; this growth is described by the monotonically and continuously increasing diameter $a(t)$. At first the particles move freely and without collisions because of their small size, but as they grow, collisions become more frequent. This process continues in principle until the collision rate diverges, the stage at which jamming occurs.

The collision dynamics for the expanding particles is nonconservative. Velocity components for a colliding pair transverse to the line of centers at contact are unchanged by the collision. However, the outgoing velocity components along the line of centers receive an increment equal to $a'(t)$, and consequently the kinetic energy of the system discontinuously increases at each collision. This phenomenon is a significant contributor to the diverging collision rate at jamming, as the following heuristic argument shows.

Consider a rigid particle system just prior to the instant ($t = t_p$) that it jams up in a packing with particle diameter a_p. Let $v(t)$ and $R(t)$ respectively stand for the mean particle speed and collision rate at time $t < t_p$. These two quantities are related through the average distance traveled between collisions, so we can write

$$R(t) = K_1 v(t)/[a_p - a(t)] \tag{3.1}$$

where K_1 is a positive constant of order unity. As already mentioned, the collision dynamics of expanding particles is nonconservative, and each collision [for $v(t)$ already large] increments the speed by an amount proportional to the rate of expansion $a'(t)$. Consequently

$$v'(t) = K_2 R(t)\, a'(t) \tag{3.2}$$

where K_2 is another order-unity positive constant.

Since we are concerned with the limiting approach of t to t_p, it is sufficient to treat the diameter growth rate as a constant, say a_0. In that event, $R(t)$ may be eliminated from Eqs. (3.1) and (3.2) to yield

$$v'(t) = K_1 K_2 v(t)/(t_p - t) \tag{3.3}$$

which integrates to

$$v(t) = v_0 (t_p - t)^{-K_1 K_2} \tag{3.4}$$

where v_0 is set by the initial velocity distribution. Notice that a_0 has dropped out of this result. However, the computationally more significant collision rate is inversely proportional to a_0:

$$R(t) = (K_1 v_0/a_0)(t_p - t)^{-(K_1 K_2 + 1)} \tag{3.5}$$

The quantities K_1 and K_2 can be expected to depend significantly on dimension D, because the number of nearest neighbors varies strongly with D. For given D they can also depend (more weakly) on the specific packing geometry involved.

The simplest diameter growth rule is obviously the constant rate:

$$a(t) = a_0 t \qquad (t \geqslant 0) \tag{3.6}$$

The t_p will then be inversely proportional to a_0, suggesting use of a rescaled time variable $\tau = a_0 t$. The collision rate $R_0(\tau) = R(t)$ in this more natural variable then becomes

$$R_0(\tau) = K_1 v_0 a_0^{K_1 K_2} (\tau_p - \tau)^{-(K_1 K_2 + 1)} \tag{3.7}$$

The inevitable divergence of collision rate at jamming has obvious numerical consequences. The strict jamming limit is never quite attained, but only a lower limit (in time, particle diameter, covering fraction) that is enforced by finiteness of computing resources. As a practical matter, not expected to affect the outcome in a significant way, particle velocities can be renormalized repeatedly during late stages of the concurrent construction calculations to relieve (but not eliminate) numerical divergence.

In the slow-particle-expansion limit [compared to mean speed: $a'(t) \ll v(t)$] the system of particles can be expected to sample ergodically the accessible configuration space, at least for $D > 1$.[15] However, this is not sufficient to ensure that equilibrium strictly be attained. The latter would guarantee that any finite-N system would inevitably end up in the most densely packed structure, in the slow-diameter-expansion limit. In fact such an outcome becomes increasingly unlikely as N increases. The explanation lies in the disconnection phenomenon noted in Section 2 for the available configuration space region $S(a)$. Each time such a disconnection occurs there will be probabilities q and $1-q$, respectively, for being trapped in one of the fragments and in its complement. For the slow-particle-expansion limit with ergodic sampling just before disconnection, these will be proportional to the contents of the fragment and its complement, and as both such contents will be positive at disconnection, both q and $1-q$ lie between 0 and 1.

In order for the system to attain any given packing p (we do not distinguish arrangements that differ only by particle permutations), it must survive the correct sequence of branchings at all encountered fragmentations on the way to jamming. The overall survival probability for this sequence (indexed by j) can be written as the product

$$Q_p = \prod_j q_j < 1 \tag{3.8}$$

In particular this applies to the densest possible packing. With large N the number of factors in Eq. (3.8) will likewise be large, causing Q_p to be very small. For large N the number of "traps" is very large into which the system might fall on the way to densest packing.

If the particle expansion rate is large, the bifurcation probabilities q and $1-q$ would no longer exactly equal the respective region contents. However, somewhat modified probabilities dependent on $a(t)$ will exist, still lying in the range (0, 1). The preceding argument qualitatively still applies; random initial conditions can only rarely be expected to produce the densest possible packing when N is large.

4. DISK PACKINGS

Disk packings are created by expanding N particles within a square cell with periodic boundary conditions. The initial stages of the concurrent construction employ a constant diameter growth rate as shown in Eq. (3.6), and this initial rate typically is maintained until $(t_p - t)/t_p < 10^{-3}$, so that the system of disks is nearly in its final jammed structure. An important issue is how the distribution of results depends on a_0 in Eq. (3.6).

A substantial fraction of our disk-packing studies to date have involved $N = 2000$. The geometric properties of these relatively large systems are complex, and it seems to be helpful for interpretation purposes also to examine the behavior of selected small systems. In particular, ref. 1 stressed that the case $N = 27$ provided a convenient prototype for observation of "rattler" disks.

It is in the same spirit that we now briefly examine the $N = 56$ case. This is particularly instructive because of the near fit of the square cell with the close-packed triangular array of disks. Notice that the horizontal and vertical dimensions, respectively, of 8 rows of 7 disks are $7a$ and $4\sqrt{3}\,a$, with ratio

$$\frac{4\sqrt{3}}{7} = 0.98974... \tag{4.1}$$

If hypothetically the 56 disk centers were arranged in a triangular crystal aligned with the square cell, and uniaxially strained along the "short" direction to fit seamlessly with periodic images, diameter growth would produce contact between all neighbor pairs just along rows. A simple calculation shows that this would occur when the covering fraction is

$$\xi = \frac{2\pi}{7} = 0.8975979... \tag{4.2}$$

But clearly this is not an optimal arrangement, and indeed not even a packing by the definition given in Section 2. The rows of particles could be buckled to eliminate the contacts, permitting further particle growth and an increase in ξ. Just how this buckling should occur to maximize ξ is not immediately obvious.

In ten independent trials, each with $a_0 = 10^{-3}$, the same final packing of 56 disks appeared (aside from symmetry operations of translation, 90° rotation, and inversion). The covering fraction was found to be

$$\xi = 0.898059591... \tag{4.3}$$

Figure 3 displays the structure, with bonds included to show particle contacts (numerically these are identified by particle surfaces closer than

10^{-7} of the diameter). In addition, contact triangles have been shaded for clarity. The small increase of ξ in Eq. (4.3) over the value in Eq. (4.2) represents the buckling advantage. Figure 3 shows that the extent of buckling is small, so superficially the disk pattern strongly resembles that of a perfect crystal. However, the detailed buckling pattern and set of contacts are not simple, so it seems surprising that essentially the same result should occur in all ten trials. It also seems surprising that none of the 56 particles experience 6 neighbor contacts; 16 contact 3 neighbors, 20 contact 4 neighbors, and 20 contact 5 neighbors.

The arrangement in Fig. 3 is not the only 56-disk packing. We have also created some lower-density examples ($\xi \cong 0.8427$) by packing 57 disks and then removing one of its several disks with six contacts to leave a vacancy. Others have been directly produced by rapid expansion ($a_0 = 100$ initially) of 56 disks.

The packing geometry illustrated in Fig. 3 for 56 disks can be expected to have relevance to at least some packings of larger numbers of disks. The requirement that a reasonably well-ordered grouping of particles fit tightly

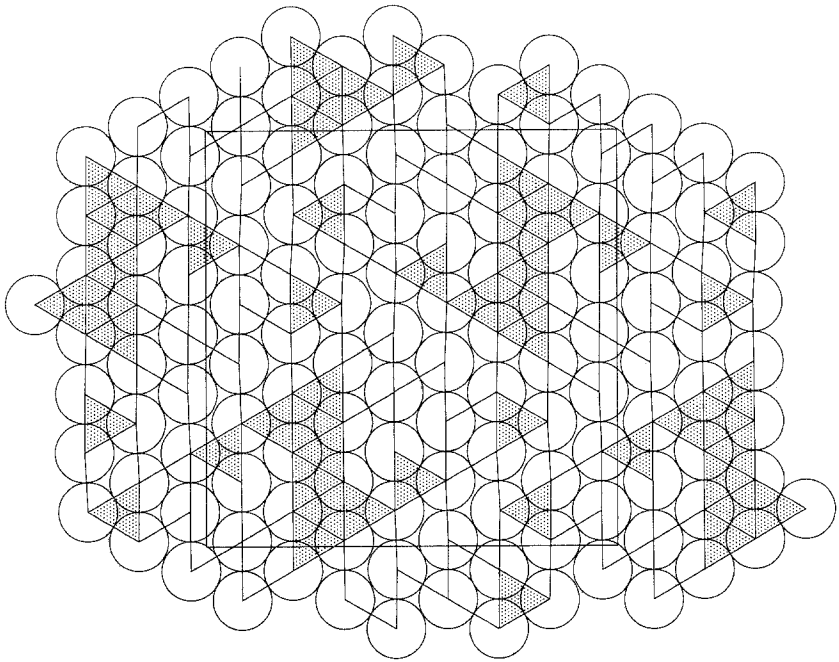

Fig. 3. Packing of 56 disks in a square cell with periodic boundary conditions ($\xi = 0.898059591...$). Disk pair contacts are indicated as bonds between centers, and contact triangles have been shaded.

with its surroundings (in this case its own periodic images) can have a significant distorting effect. Pair contacts, always sixfold in a perfect crystalline array, can be broken in a complex pattern with only a small reduction in local covering fraction.

Figures 4–7 present examples of 2000-disk packings. The initial growth rates employed in their concurrent constructions span five orders of magnitude: $a_0 = 10^{-3}$ for Figs. 4 and 5, $a_0 \cong 3.2$ for Fig. 6, and $a_0 = 10^2$ for Fig. 7. All four structures can be described as polycrystalline, in agreement with our earlier observations reported in ref. 1. Figures 4–7 also illustrate with vivid visual impact the trend toward greater packing irregularity with increasing initial growth rate a_0, and consequent reduction in average crystalline grain size. The mean grain size for the slowly grown cases in Figs. 4

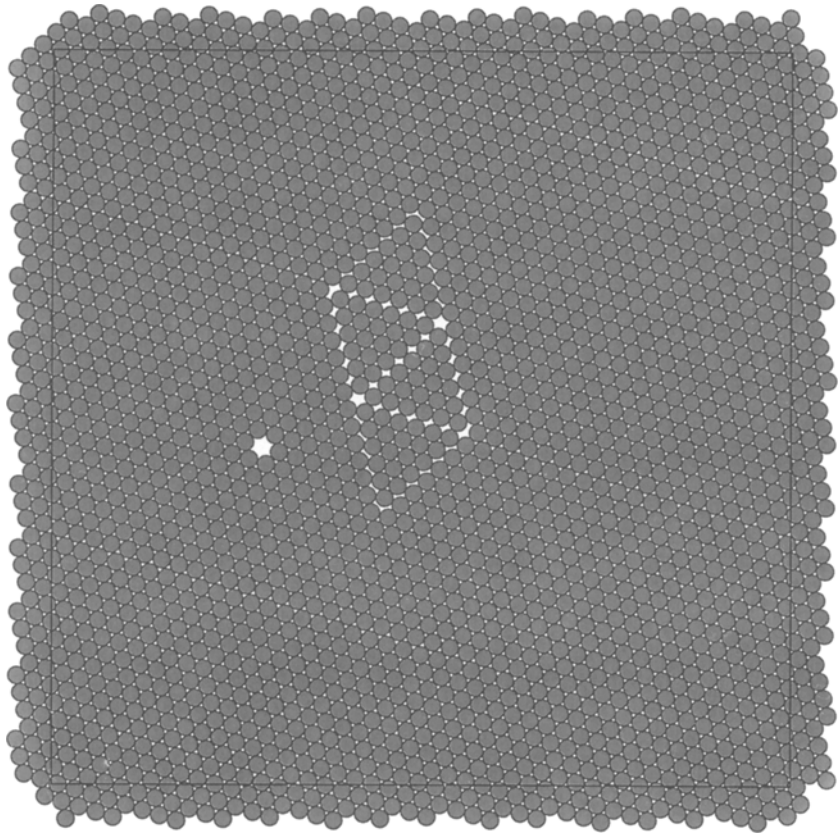

Fig. 4. Packing of 2000 disks in a square cell with periodic boundary conditions. The initial growth rate was $a_0 = 10^{-3}$, and the final covering fraction is $\xi = 0.901184607$.

and 5 is comparable to the size of the entire cell itself, but is considerably smaller in the rapidly-grown packing in Fig. 7. As should consequently be expected, the densities (covering fractions) of slowly grown arrangements tend to be higher than those grown rapidly.

These observations can be transferred to statements about the branching probabilities that appear in Eq. (3.8). Large growth rates bias the q_j in favor of irregular, highly defective, packings at the expense of the more regular packings.

The structures shown in Figs. 4–7 illustrate some of the same disk-packing features observed earlier.[1] These include vacancies and linear shear fractures appearing within otherwise well-ordered regions,

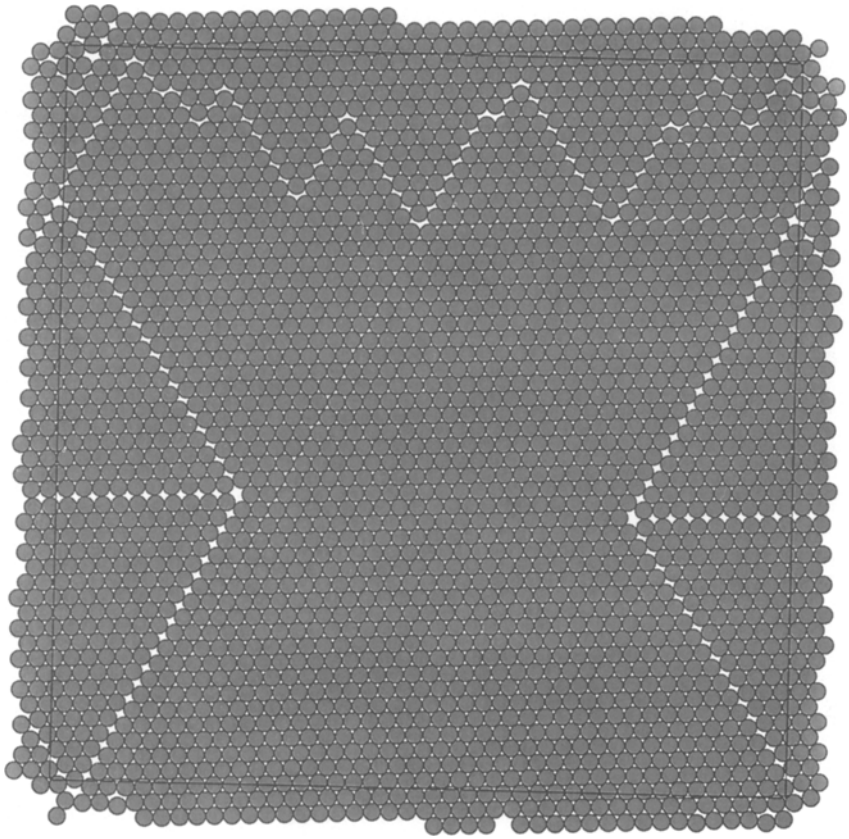

Fig. 5. Packing of 2000 disks created with initial growth rate $a_0 = 10^{-3}$. The final packing fraction is $\xi = 0.895010191$.

and "rattler" disks which are normally found within grain boundaries. Examples of the latter are highlighted in Figs. 6 and 7 as unshaded circles.

The presence of crystalline grains as a predominant textural feature in disk packings has a strong influence on the pair correlation function $g(r)$. Figure 8 shows a plot in histogram form of the $g(r)$ for the packing exhibited in Fig. 6. By convention $g(r)$ is normalized to unity for a random distribution of particle positions. The obvious characteristics shown for $g(r)$ in Fig. 8 are the strong isolated peaks with a low background "noise." The peaks are to be associated with the neighbor distances in the perfect triangular array:

$$r/a = (m^2 + mn + n^2)^{1/2} \tag{4.4}$$

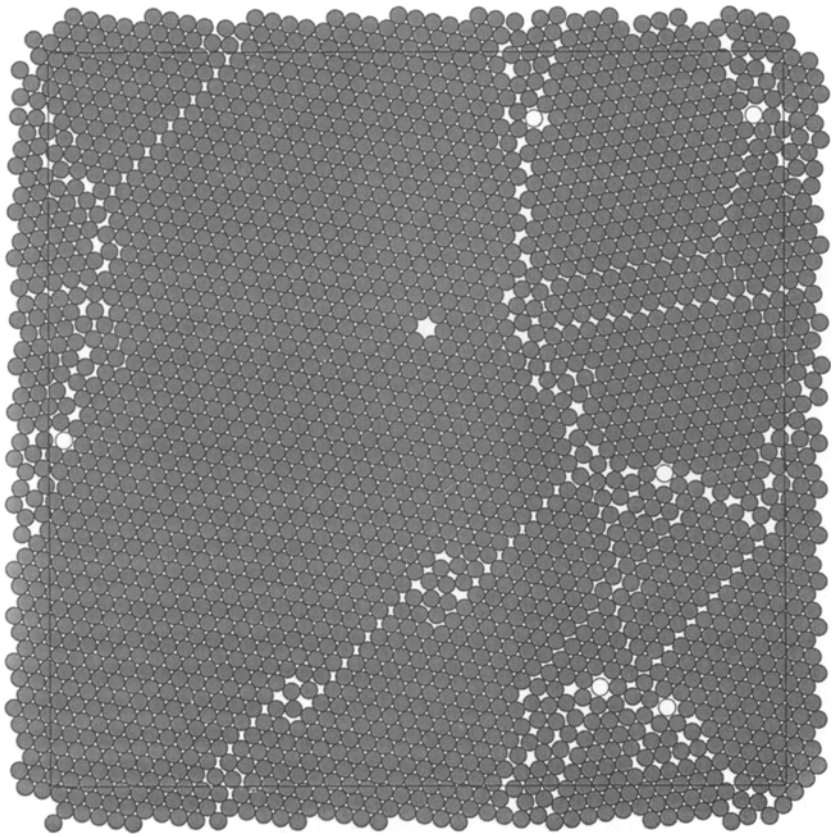

Fig. 6. Packing of 2000 disks with initial growth rate $a_0 \cong 3.2$. The final packing fraction is $\xi = 0.882965548$.

where m and n are integers (positive, negative, or zero). In more irregular packings the large-distance peaks tend to be substantially lower, and the "background" enhanced.

Using once again the numerical criterion that two disks are counted as contacting if their surfaces are within 10^{-7} of the diameter, the 2000 disks in Figure 6 have been classified by the number of contacts they experience. Figure 9 exhibits the results. The most frequent contact number is the maximum possible, six. The relatively high occurrence frequencies for contact numbers 5, 4, and 3 rests largely on the behavior illustrated earlier for 56 disks in Fig. 3, namely that the fitting requirements can distort a grain to create a complex pattern of broken contacts. Indeed a detailed study of the locations in the packing of Fig. 6 of particles with various

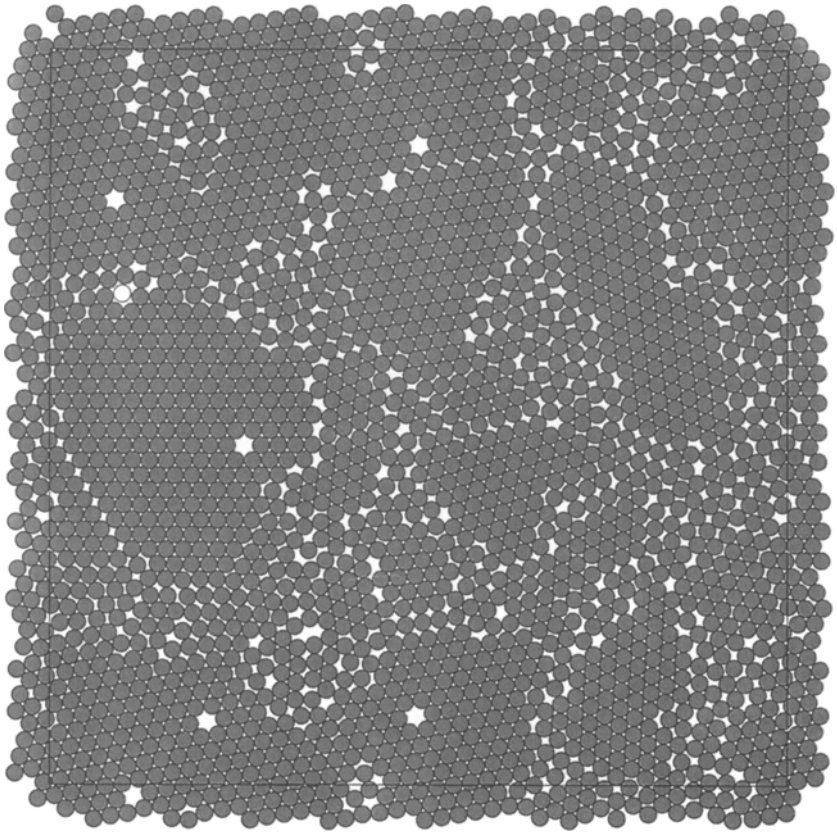

Fig. 7. Packing of 2000 disks with initial growth rate $a_0 = 10^2$. The final packing fraction is $\xi = 0.852116396$.

contact numbers seems to verify that this is so. The relatively small number of particles with 2, 1, or 0 contacts are those free to rattle, either in isolation or in a small contiguous group.

5. SPHERE PACKINGS

The disk-packing results reported in ref. 1 and in Section 4 provide a background against which rigid sphere results can be evaluated. We have studied the concurrent formation of sphere packings in cubic cells with periodic boundary conditions, using 1000 and 8000 particles.

Figure 10 displays a packing of 1000 spheres, prepared with initial diameter growth rate $a_0 = 1.0$. Its covering fraction is $\xi = 0.63715960$. Examination of this picture fails to reveal any polycrystallinity that was so

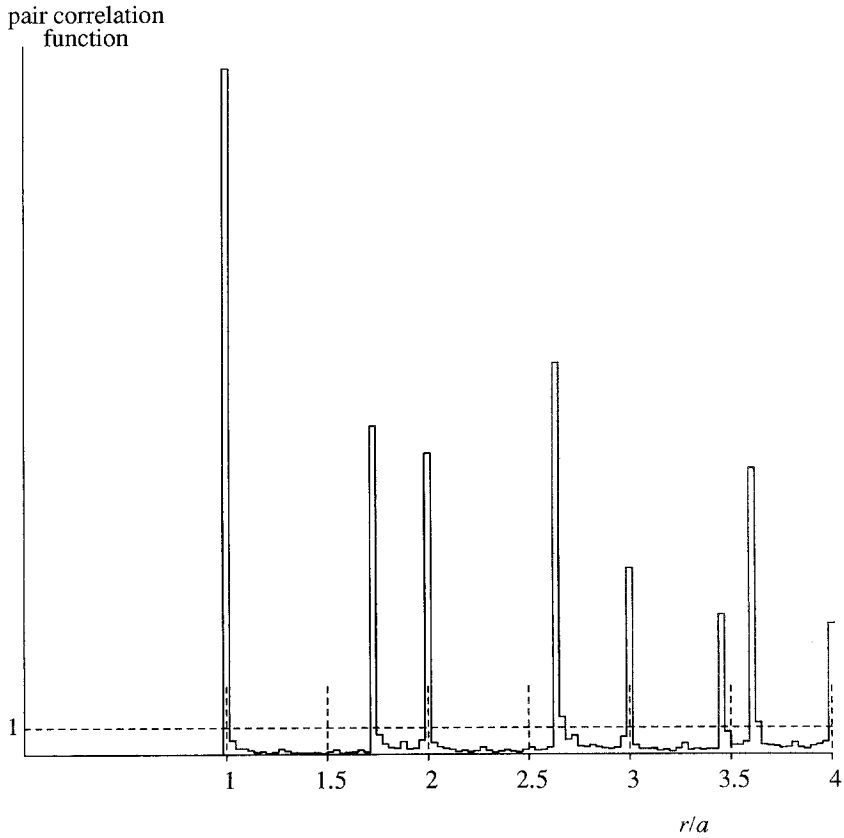

Fig. 8. Pair correlation function for the disk packing illustrated in Fig. 6.

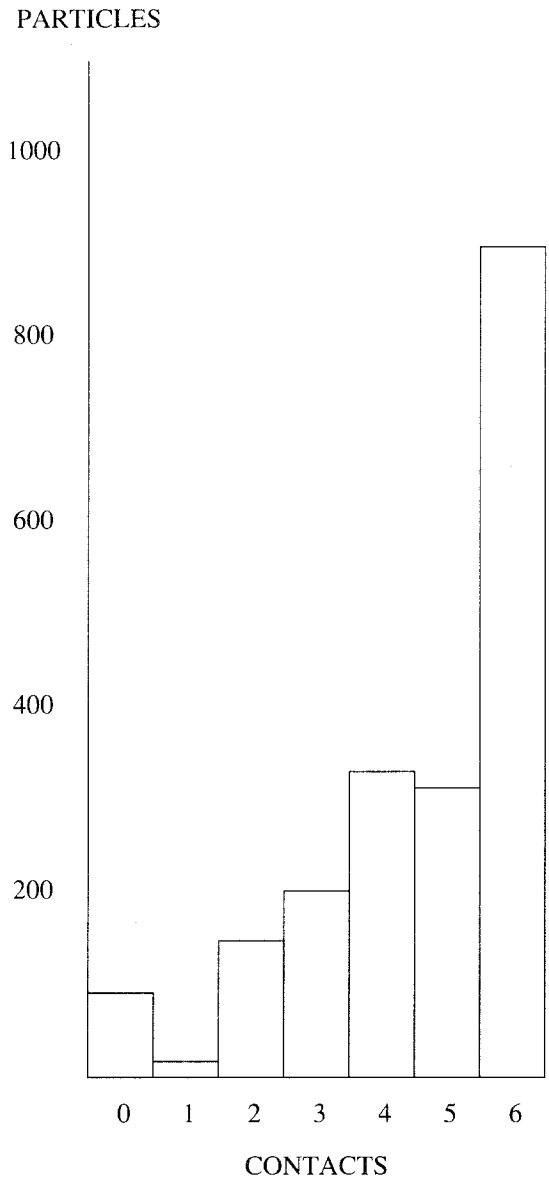

Fig. 9. Histogram of numbers of disks in Fig. 6 with various contact numbers.

obvious in the rigid disk packings (Figs. 3–7). The structure is more uniformly irregular. This observation in fact applies to all sphere packings created to date by our concurrent construction method, with a_0 values in the range 10^{-3} to 10^{+2}.

This contrast in texture between the $D=2$ and $D=3$ packings is dramatically reflected in the contrast between pair correlation functions. Figure 11 shows the pair correlation function $g(r)$ for an 8000-sphere random packing. Its overall form agrees qualitatively with those that have been reported from previous sphere packing investigations.[2–7] A very large peak appears at contact of course, because the spheres are jammed. But unlike the disk $g(r)$ shown earlier in Fig. 8, no subsequent peaks of comparable magnitude appear. The sphere result in Fig. 11 does, however,

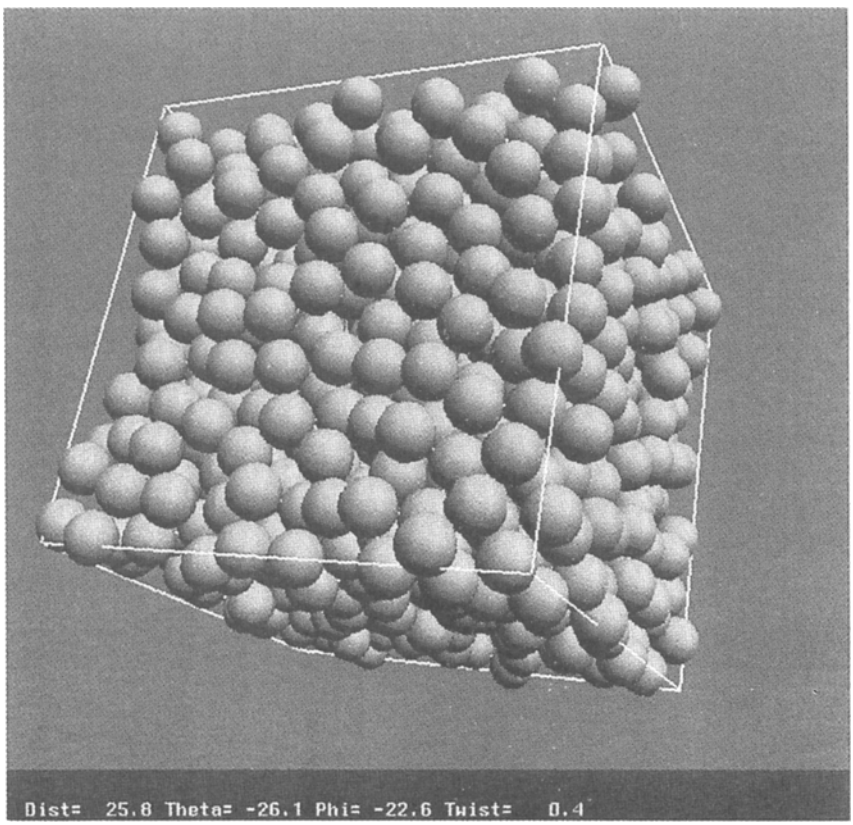

Fig. 10. Packing of 1000 rigid spheres in a cube, subject to periodic boundary conditions. The initial diameter growth rate was $a_0 = 1.0$, and the final covering fraction is $\xi = 0.63715960$.

exhibit the split second peak that has often been mentioned as a characteristic signature of short-range order in amorphous media.[16] At even larger separations the sphere $g(r)$ has gentle decaying oscillations about the asymptotic value unity.

The distribution of spheres by contact number has been calculated for the 8000-particle packing upon which Fig. 11 is based. The same "10^{-7} diameter" criterion as before has been used. The results are presented as a histogram in Fig. 12. Geometrically it is possible for a sphere simultaneously to touch 12 others (as in fcc and hcp crystals, as well as

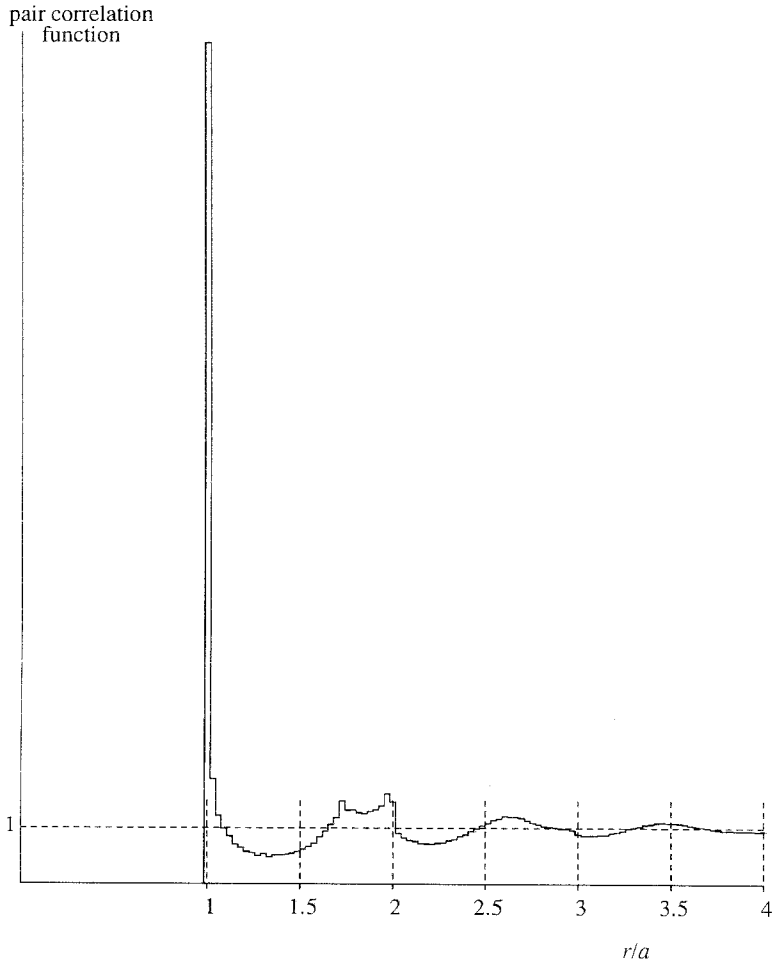

Fig. 11. Pair correlation function $g(r)$ for an 8000-sphere irregular packing. The initial growth rate was $a_0 = 1.0$ and the final packing fraction is $\xi = 0.63788205$.

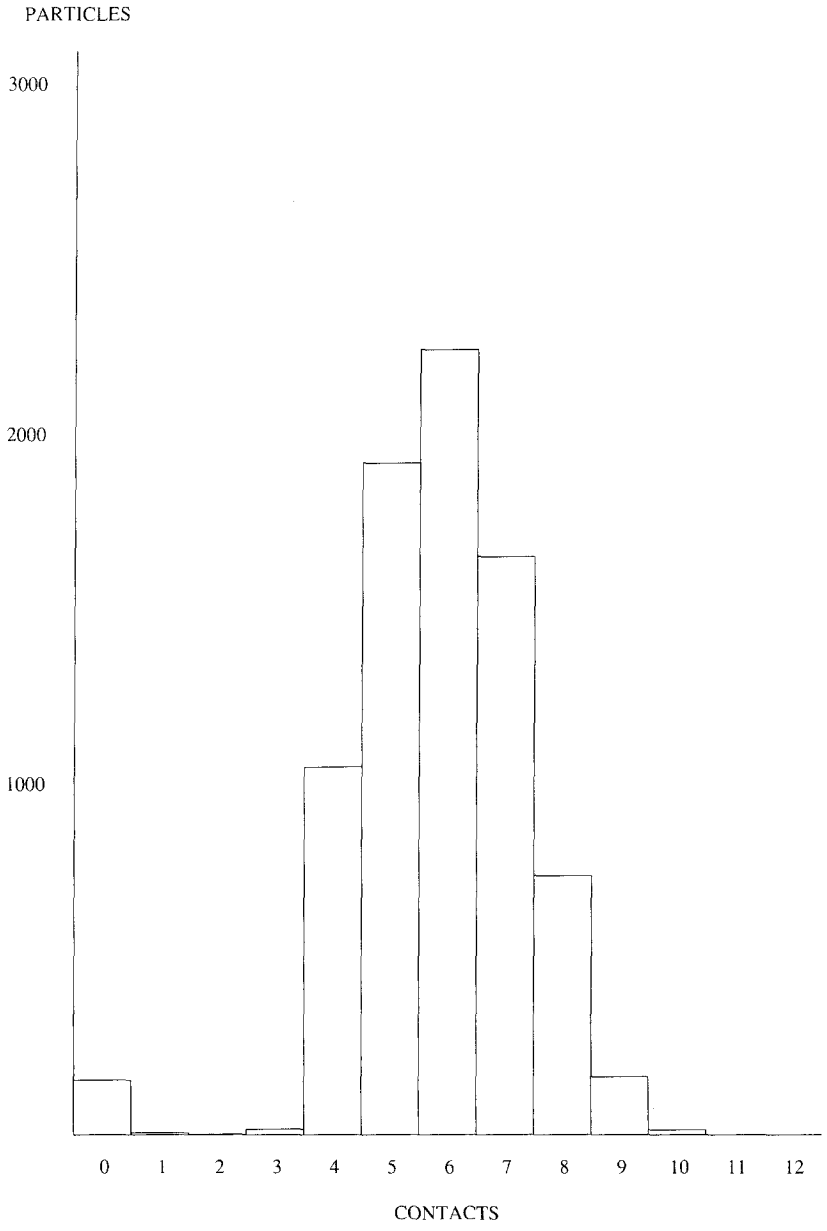

Fig. 12. Distribution of contact numbers for the 8000-sphere packing upon which Fig. 11 is based.

icosahedral clusters). But none of the 8000 spheres experience 12 or even 11 contacts; 10 is the largest contact number observed, and is realized only by 14 spheres. This three-dimensional characteristic is quite unlike that illustrated by Fig. 9 for rigid disks, where the maximum possible contact number is also the most probable.

The mean contact number in Fig. 12 is 5.8295. The contacts are spatially organized so that on average 1.80825 contact triangles pass through any sphere as vertex. However, a surprisingly small average number of contact tetrahedra, 0.0145, employ any given sphere as a vertex, a result unlikely to emerge from a sequential construction procedure.

The results in Fig. 12 reveal the presence of a substantial number of rattler spheres. Specifically, the numbers of particles with 0, 1, 2, and 3 con-

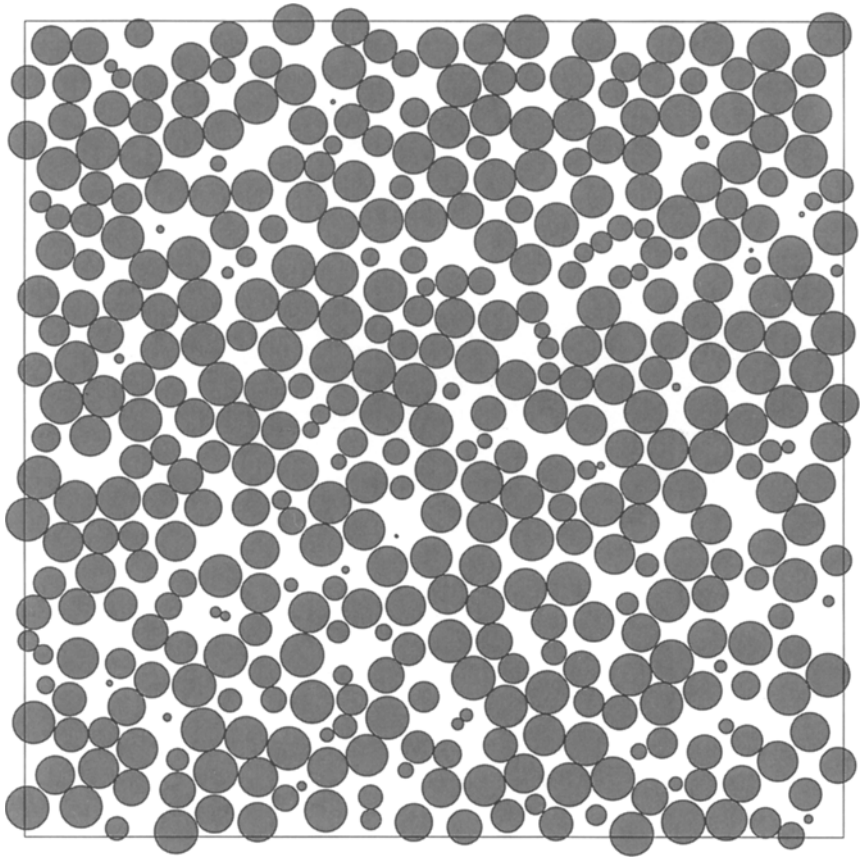

Fig. 13. Planar slice through an 8000-sphere irregular packing, parallel to a face of the periodic cell. Shaded circles represent loci of points interior to spheres.

tacts are 158, 6, 2, and 16 respectively, all of which must be unjammed in the packing. Obviously the inclusion of rattler particles is an attribute shared by irregular packings in two and in three dimensions.

On the basis of limited sampling it appears that rattler spheres tend to be rather uniformly distributed throughout their irregular host packings. Since those packings do not display a polycrystalline texture, there is nothing analogous to the disk-packing observation that rattlers in two dimensions are confined to grain boundaries.[1]

Figures 4, 6, and 7 show obvious examples of monovacancies occurring within ordered crystalline grains. In view of nonoccurrence of crystalline grains in the three-dimensional packings, one might reasonably surmise that such discrete voids would be absent for spheres. Indeed that appears to be the case. The volume uncovered by spheres in any three-dimensional packing is multiply connected and complicated, yet may be studied as a sequence of slices normal to, and closely spaced along, any selected direction. Figure 13 shows an example of one of these slices, taken through an irregular 8000-sphere packing. Sequences of these views fail to show clear-cut cases of monovacancies, and strengthen the inference that irregular sphere packings are essentially devoid of crystallites.

The density range attained by our concurrent construction of sphere packings is relatively narrow:

$$0.63 \leqslant \xi \leqslant 0.65 \qquad (D = 3) \tag{5.1}$$

There appears to be a weak tendency for the final ξ to increase with decreasing a_0; however, the statistical variations from one case to the next with fixed a_0 tend to obscure this trend somewhat. Note that the range in Eq. (5.1) is a substantially smaller fraction of the close-packed maximum ($\xi = 0.7404...$) than is the corresponding disk-packing range attained

$$0.85 \leqslant \xi \leqslant 0.90 \qquad (D = 2) \tag{5.2}$$

in comparison with its close-packed maximum ($\xi = 0.9068...$).

6. DISCUSSION

The disk and sphere irregular packings created by our concurrent construction method present clear-cut contrasts that illustrate the importance of spatial dimension D. The trivial case $D = 1$ provides one extreme, with only the long-range-ordered periodic packing, and $\xi = 1$. Upon increasing D to 2, packing diversity becomes possible, but even rapidly grown irregular packings exhibit a polycrystalline texture and substantial short- to intermediate-range order. However, when D increases to 3 no substantial

crystalline short-range order is present; typical irregular sphere packings are uniformly disordered.

It would be desirable to extend the study to $D=4$. In particular the presence of rattler particles, observed thus far in $D=2$ and $D=3$, would be an obvious focus of attention. However, the corresponding computations would be very demanding. We suspect that more than 10^4 hyperspheres would have to be considered to infer "bulk" packing properties, and the larger number of neighbors in this higher dimension would tend to slow down the procedure even on a per-particle basis.

The enumeration of hard particle packings remains an open problem. It is reasonable to suppose that the number of distinct packings $\Omega_d(N, D)$ for N particles in D dimensions is asymptotically exponential in N:

$$\ln \Omega_d(N, D) \sim \alpha(D)\, N \qquad (N \to \infty) \tag{6.1}$$

All one knows for certain is that $\alpha(1)$ vanishes. Nevertheless one might postulate the following:

$$0 = \alpha(1) < \alpha(2) < \alpha(3) < \alpha(4)... \tag{6.2}$$

citing the noncrystallinity of sphere packings ($D=3$) as evidence that many more geometric options are available for packing than with disks ($D=2$).

An issue apparently untouched in all random disk or sphere packing studies to date is the nature of the interface between macroscopic crystalline and amorphous regions. An extension of our approach could be formulated to handle this case. Particles of the crystalline portion could be held fixed in both position and size while the amorphous portion would be grown as discussed above. The fixed crystalline substrate particles would initially have to be shielded from invasion by the initially small particles of the amorphous set. Later, both sets of particles could grow in step till jamming occurred. The resulting inhomogeneous packings could be surveyed to determine the width and character of the transition zone.

Lastly, we mention the obvious extension to mixtures of disks or of spheres with different sizes. This simply requires introduction of separate time-dependent diameter functions $a_v(t)$ for each species v. It seems obvious that presence of a minor fraction of small particles compared to the rest all of larger size will mainly produce rattlers. This should be particularly noticeable for $D=2$, and the small-particle rattlers would not be confined to grain boundaries. But when roughly equal numbers of small and of larger particles are present, the nature of the packings is not obvious and deserves study. In particular the dependence of results on expansion rate may be particularly significant because of segregation processes.

ACKNOWLEDGMENT

We thank Prof. Zoltan Furedi for correcting an error in an earlier version of this paper.

REFERENCES

1. B. D. Lubachevsky and F. H. Stillinger, *J. Stat. Phys.* **60**:561 (1990).
2. C. H. Bennett, *J. Appl. Phys.* **43**:2727 (1972).
3. D. J. Adams and A. J. Matheson, *J. Chem. Phys.* **56**:1989 (1972).
4. W. M. Visscher and M. Bolsterli, *Nature* **239**:504 (1972).
5. A. J. Matheson, *J. Phys. C* **7**:2569 (1974).
6. P. Mrafko and P. Duhaj, *Phys. Stat. Sol. (a)* **23**:583 (1974).
7. T. Ichikawa, *Phys. Stat. Sol. (a)* **29**:293 (1975).
8. F. Delyon and Y. E. Lévy, *J. Phys. A* **23**:4471 (1990).
9. G. Mason, *Disc. Faraday Soc.* **43**:75 (1967).
10. J. L. Finney, *Mater. Sci. Eng.* **23**:199 (1976).
11. E. L. Hinrichsen, J. Feder, and T. Jossang, *Phys. Rev. A* **41**:4199 (1990).
12. B. D. Lubachevsky, *J. Comp. Phys.* **94**:255 (1991).
13. H. L. Frisch, *Adv. Chem. Phys.* **6**:229 (1964).
14. F. H. Stillinger and Z. W. Salsburg, *J. Stat. Phys.* **1**:179 (1969).
15. D. Ruelle and Ya. G. Sinai, *Physica* **140A**:1 (1986).
16. J. L. Finney, *Nature* **266**:309 (1977).